

Natural Vibration Analysis of Axially Graded Tapered Rayleigh Beams on a Quadratic Bi-Parametric Elastic Foundation

O. T. Olotu^{1*}, E. O. Omole², R. O. Folaranmi³, B. M. Yisa¹, P. O. Adeniran¹, J. A. Gbadeyan¹



¹Department of Mathematics, University of Ilorin, Ilorin, Kwara State, Nigeria.

²Department of Physical Sciences, Landmark University, Omu-Aran, Kwara State, Nigeria.

³Department of Mathematical and Computer Science, Thomas Adewumi University, Oko, Kwara State, Nigeria.



ABSTRACT: Understanding the dynamic behaviour of non-homogeneous beams on elastic foundations is vital for ensuring the stability and safety of engineering structures such as bridges, buildings, and mechanical systems. This study aims to address this problem by investigating the natural vibration characteristics of such beams. The mechanical properties of the beam and the foundation stiffness are assumed to vary along the longitudinal direction. Two boundary conditions-clamped-free and clamped-clamped are considered. The differential transform method (DTM) is employed to solve the governing equation of motion, providing a numerical approximation of the beam's dynamic behaviour. The results, presented in both tabular and graphical formats, highlight the influence of key parameters such as the inverse of the slenderness ratio, foundation stiffness, and boundary conditions on the free vibration response. The findings indicate that increasing foundation stiffness leads to higher natural frequencies, with the Pasternak foundation yielding the highest values. Additionally, an axially functionally graded Rayleigh beam on a Pasternak foundation exhibits superior natural frequencies compared to a similar beam on a Winkler foundation. The effectiveness and accuracy of the DTM are further validated through two illustrative dynamic response problems, with results demonstrating excellent agreement with existing literature.

KEYWORDS: Natural vibration, functionally graded beam, differential transform method, dimensionless frequency, Rayleigh beam theory

[Received Jan. 29, 2025; Revised Feb. 28, 2025; Accepted Mar. 7, 2025]

Print ISSN: 0189-9546 | Online ISSN: 2437-2110

I. INTRODUCTION

Over the past few years, researchers have shown great interest in investigating the stationary and kinetic response of Functionally Graded (FG) beams. The concept of FGMs originated in Japan in 1984 as a means of creating heat-resistant materials. Research on FGMs is growing exponentially due to their ability to meet specific material requirements, overcoming limitations of traditional non-heterogeneous and layered composite materials. Functionally Graded Materials are heterogeneous materials employed in designing structures that withstand high temperatures. FGMs are metal-matrix composites characterized by gradual changes in material ratios, typically consisting of ceramic and metal alloy blends. The ceramic component offers high thermal resilience as a result of its low heat conductivity, while the deformable metal component avoids breakage resulting from stresses generated from rapid temperature changes. FGMs are high-tech materials with physical-mechanical parameters that vary continuously with respect to position or distance. Their usage in load-bearing structures leads to stress relief, improved strength, and toughness. FGMs have become increasingly useful in high-tech transportation, defense industries, nuclear reactors, and electronics.

Understanding the vibrational behaviour of beams is essential for their safe and efficient operation in

various engineering applications. Unlike traditional beams with uniform material properties, Axially Functionally Graded (AFG) beams allow continuous variation in properties such as density and elasticity along their length, enabling engineers to optimize strength and weight for specific applications (Aydogdu & Taskin, 2007). Tapered beams, with their non-uniform cross-section, further enhance structural efficiency by reducing weight while maintaining integrity (Simsek, 2010)

Vibration analysis is crucial in dynamic environments, where natural frequencies significantly influence structural performance. The application of Functionally Graded Materials (FGMs) has gained prominence in meeting stringent engineering demands, particularly under extreme thermal or environmental conditions (Shahba et al., 2011; Alshorbagy et al., 2011). Researchers have thoroughly investigated the free vibration of FGM structures, with specific focus on beams, the fundamental building blocks of engineering systems. While popular beam theories like Euler-Bernoulli and Timoshenko have been widely used, Rayleigh beam theory, that accounts for the influence of rotatory inertia, is particularly relevant for analyzing micro - and nano-scale beams (Avcar & Alwan, 2017; Kumar, 2022).

*Corresponding author: olotu.ot@unilorin.edu.ng

Elastic foundations provide a realistic model for beam supports in engineering applications. The quadratic bi-parametric foundation model extends simpler elastic foundation theories by incorporating two stiffness parameters: one for deflection and another for rotational resistance. This model offers a more accurate representation of real-world support conditions (Catal, 2007; Chen et al., 2021). Previous studies have investigated dynamic analysis of FGM beams under various configurations and conditions. For example, Navier solutions have been applied to simply supported beams (Aydogdu & Taskin, 2007), higher-order theories have been explored (Simsek, 2010), and finite element methods have been employed for stability and free vibration analysis (Shahba et al., 2011; Alshorbagy et al., 2011). Additionally, semi-analytical approaches such as the Adomian Decomposition Method have been used to address challenges posed by variable coefficients (Cogkun et al., 2014).

Recent research has extended vibration analysis to specialized cases. Avcar & Alsaied (2017) studied free vibrations of FGM Rayleigh beams with variable characteristics, while Ebrahimi-Mamaghani et al. (2020) investigated both free and forced vibrations under moving loads. Lamprea-Pineda et al. (2022) extended beam theories to multi-layered and periodic structures like railway tracks, and Chen et al. (2021) analyzed the out-of-plane bending vibrations of tapered Rayleigh beams. Kumar (2022) employed Timoshenko beam theory and Hamilton's principle for analyzing FGM beams, further emphasizing the versatility of advanced methods in beam vibration analysis. Integral Numerical Method was employed by Sulaiman et al., (2024) to analyze the vibration characteristics of slender beams with presence of viscous damping coefficient resting on elastic foundation.

Beyond these traditional methods, the Differential Transform Method (DTM) has emerged as a robust semi-analytical technique for addressing linear and nonlinear differential equations. Originally developed for electrical circuit analysis (Zhou, 1986), DTM has been successfully applied to structural dynamics problems (Malik & Dang, 1998). Catal (2007) used DTM to analyze beams on elastic soil, while Mei (2008) applied it to find the natural frequencies and lateral vibrations of rotating beams. Wattanasakulpong

(2012) studied the natural vibration of FGMs using DTM, and Olotu et al. (2023) studied the impact of varying subgrade properties on the frequencies of non-uniform Rayleigh beams.

Ma et al., (2024a) examined both forced and free vibrations of finite beams taking into account a moving concentrated force. The authors analyzed how three key factors - soil damping, soil mass, and subgrade modulus influence on the vibrational characteristics of slender beams. Their findings revealed that a significant increase in soil mass substantially altered the vibration behaviour of the entire system. Ma et al., (2024b) investigated how soil with finite depth affected the dynamic behaviour of a multi-span continuous beam supported by an elastic bedding. The study's results indicated that the inertial movement of soil with limited thickness had a profound impact on the continuous beam, significantly reducing its natural frequency and amplifying its resonance effect. Moreover, an increase in the subsoil reaction coefficient raises the system's fundamental frequency thus reducing the beam's deflection behaviour.

This study addressed a key research gap by analyzing the natural vibrations of AFG tapered Rayleigh beams on quadratic bi-parametric support systems, a topic largely unexplored in existing literature. By combining AFG material properties, tapered geometry, Rayleigh beam theory, and advanced foundation modelling, the study provided a comprehensive mathematical framework. Employing the differential transform method (DTM), the governing differential equations with variable coefficients were transformed into algebraic equations, enabling efficient computation of natural frequencies. The analysis, which incorporated varying slenderness ratios and foundation parameters, revealed new perspectives and deeper understandings on the vibrational behaviour of AFG tapered beams. The continuous variation of material properties, such as mass density and modulus of elasticity, through the beam's thickness was a critical aspect of the model. This work fills a significant knowledge gap in FG beam vibration analysis and offers valuable insights for researchers and engineers working with advanced beam configurations and elastic foundation systems.

II. MODEL ANALYSIS

The motion equation of a finite-length, elastically restrained AFG tapered Rayleigh beam supported by a Pasternak foundation is given by the fourth order partial differential equation Olotu *et al.* (2023),

$$\frac{\partial^2}{\partial x^2} \left[E(x)I(x) \frac{\partial^2 y(x, t)}{\partial t^2} \right] + \rho(x)A(x) \frac{\partial^2 y(x, t)}{\partial t^2} - \frac{\partial}{\partial x} \left[N(x) \frac{\partial y(x, t)}{\partial x} \right] - \frac{\partial}{\partial x} \left[\rho(x)I(x) \frac{\partial^2 y(x, t)}{\partial x \partial t^2} \right] - \frac{\partial}{\partial x} \left[G(x) \frac{\partial y(x, t)}{\partial t} \right] + K(x)y(x, t) = 0, \quad x \in (0,1) \quad (1)$$

where $y(x, t)$ denotes the dynamic response of the beam, $E(x)$, $I(x)$, and $\rho(x)A(x)$ represent the variable Young's modulus, moment of inertia, and mass per unit length respectively of the beam, $K(x)$ and $G(x)$ correspond to the variable Winkler's foundation stiffness and the shear modulus. $N(x)$ is the arbitrary variable axial tensile force which is defined by $N(x) = N_0$ for an

applied axial end force and $N(x) = \int_x^l g(\varphi) d\varphi$ when a distributed axial force $g(x)$ is exerted on the beam. $\rho(x)$ is the variable density of the beam, $A(x)$ is variable cross-section area of the beam, x is the spatial length coordinate and t is the time.

The initial conditions are

$$y(x, 0) = y_0(x), \quad \text{and} \quad \frac{\partial y(x, 0)}{\partial t} = y_0'(x) \quad (2)$$

The boundary conditions are

At $x = 0$

$$E(x)I(x) \frac{\partial^2 y(x, t)}{\partial x^2} = U_{\theta L} \frac{\partial y(x, t)}{\partial x} \quad (3)$$

and

$$\frac{\partial}{\partial x} \left[E(x)I(x) \frac{\partial^2 y(x, t)}{\partial x^2} \right] - N(x) \frac{\partial y(x, t)}{\partial x} - \rho(x)I(x) \frac{\partial^3 y(x, t)}{\partial x \partial t^2} = -U_{TL} y(x, t) \quad (4)$$

At $x = l$

$$E(x)I(x) \frac{\partial^2 y(x, t)}{\partial x^2} = -U_{\theta R} \frac{\partial y(x, t)}{\partial x} \quad (5)$$

and

$$\frac{\partial}{\partial x} \left[E(x)I(x) \frac{\partial^2 y(x, t)}{\partial x^2} \right] - N(x) \frac{\partial y(x, t)}{\partial x} - \rho(x)I(x) \frac{\partial^3 y(x, t)}{\partial x \partial t^2} = U_{TL} y(x, t) \quad (6)$$

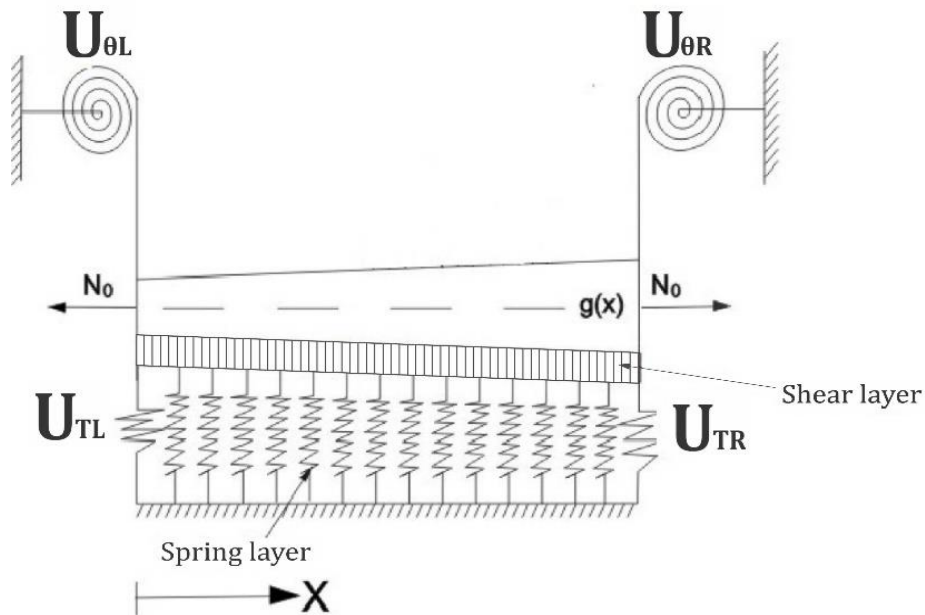


Figure 1: The model of an AFG tapered Rayleigh beam support by Pasternak's elastic foundation

where U_{TL} , $U_{\theta L}$, $U_{\theta R}$ and U_{TR} are the rotational and translational spring constants at the left and right of the beam respectively. Since natural vibration is taken into account, then the response $y(x, t)$ ensued the form

$$y(x, t) = Y(x)(a_1 \cos \omega t + a_2 \sin \omega t), \quad (7)$$

where the amplitude of vibration of the beam is $Y(x)$, the angular frequency is ω , t is the time, a_1 and a_2 are constants.

Substitute eq. (7) into eq. (1) to give

$$\begin{aligned} \frac{d^2}{dx^2} \left[E(x)I(x) \frac{d^2 Y(x)}{dx^2} \right] - \rho(x)A(x)\omega^2 Y(x) - \frac{d}{dx} \left[N(x) \frac{dY(x)}{dx} \right] \\ + \frac{d}{dx} \left[\rho(x)I(x)\omega^2 \frac{dY(x)}{dx} \right] - \frac{d}{dx} \left[G(x) \frac{dY(x)}{dx} \right] + K(x)Y(x) = 0 \end{aligned} \quad (8)$$

Also, Eq. (7) is substituted into Eqs. (3) – (6) to give

At $x = 0$,

$$E(x)I(x) \frac{d^2 Y(x)}{dx^2} = U_{\theta L} \frac{dY(x)}{dx} \quad (9)$$

and

$$\frac{d}{dx} \left[E(x)I(x) \frac{d^2 Y(x)}{dx^2} \right] - N(x) \frac{dY(x)}{dx} + \rho(x)I(x)\omega^2 \frac{dY(x)}{dx} = -U_{TL} Y(x) \quad (10)$$

At $x = l$,

$$E(x)I(x) \frac{d^2 Y(x)}{dx^2} = -U_{\theta R} \frac{dY(x)}{dx} \quad (11)$$

and

$$\frac{d}{dx} \left[E(x)I(x) \frac{d^2 Y(x)}{dx^2} \right] - N(x) \frac{dY(x)}{dx} + \rho(x)I(x)\omega^2 \frac{dY(x)}{dx} = U_{TR} Y(x) \quad (12)$$

By defining the following dimensionless parameters, we have:

$$\left. \begin{aligned}
 \xi &= \frac{x}{l}, & \beta_{\theta L} &= \frac{U_{\theta L} l}{E(0)I(0)}, \\
 y(\xi) &= \frac{Y(x)}{l}, & \beta_{\theta R} &= \frac{U_{\theta R} l}{E(l)I(l)}, \\
 s(\xi) &= \frac{E(x)I(x)}{E(0)I(0)}, & \beta_{TL} &= \frac{U_{TL} l^3}{E(0)I(0)}, \\
 n(\xi) &= -\frac{N(x)l^2}{E(0)I(0)}, & \beta_{TR} &= \frac{U_{TR} l^3}{E(0)I(0)}, \\
 r(\xi) &= \frac{\rho(x)A(x)}{\rho(0)A(0)}, & \tau_R &= \frac{s'(\xi)}{s(\xi)} \Big|_{\xi=1}, \\
 h(\xi) &= \frac{\rho(x)I(x)}{\rho(0)I(0)}, & \eta_R &= \frac{N(l)l^2}{E(l)I(l)}, \\
 \gamma &= \frac{1}{l} \sqrt{\frac{I(0)}{A(0)}}, & k(\xi) &= \frac{K(x)l^4}{E(0)I(0)}, \\
 \Lambda^2 &= \frac{\rho(0)A(0)\omega^2 l^4}{E(0)I(0)}, & g(\xi) &= \frac{G(x)l^2}{E(0)I(0)}, \\
 \psi_R &= \frac{h(\xi)}{s(\xi)} \Big|_{\xi=1}, & \alpha^2 &= \frac{\rho(0)A(0)\Omega^2 l^4}{E(0)I(0)},
 \end{aligned} \right\} \quad (13)$$

By utilizing Eq. (13), Eqs. (8) – (12) are expressed in dimensionless forms:

$$\begin{aligned}
 s(\xi) \frac{d^4 y(\xi)}{d\xi^4} + 2 \frac{ds(\xi)}{d\xi} \frac{d^3 y(\xi)}{d\xi^3} + \frac{d^2 s(\xi)}{d\xi^2} \frac{d^2 y(\xi)}{d\xi^2} + n(\xi) \frac{d^2 y(\xi)}{d\xi^2} + \frac{dn(\xi)}{d\xi} \frac{dy(\xi)}{d\xi} \\
 + \Lambda^2 \gamma^2 \left[h(\xi) \frac{d^2 y(\xi)}{d\xi^2} + \frac{dh(\xi)}{d\xi} \frac{dy(\xi)}{d\xi} \right] - g(\xi) \frac{d^2 y(\xi)}{d\xi^2} - \frac{dg(\xi)}{d\xi} \frac{dy(\xi)}{d\xi} \\
 + (k(\xi) - \Lambda^2 r(\xi)) y(\xi) = 0
 \end{aligned} \quad (14)$$

At $\xi = 0$

$$\frac{d^2 y(\xi)}{d\xi^2} = \beta_{\theta L} \frac{dy(\xi)}{d\xi} \quad (15)$$

and

$$\frac{d^3 y(\xi)}{d\xi^3} + \frac{ds(\xi)}{d\xi} \frac{d^2 y(\xi)}{d\xi^2} + [n(\xi) + \Lambda^2 \gamma^2 h(\xi)] \frac{dy(\xi)}{d\xi} + \beta_{TL} y(\xi) = 0 \quad (16)$$

At $\xi = 1$

$$\frac{d^2 y(\xi)}{d\xi^2} = -\beta_{\theta R} \frac{dy(\xi)}{d\xi} \quad (17)$$

and

$$\frac{d^3 y(\xi)}{d\xi^3} + \tau_R \frac{d^2 y(\xi)}{d\xi^2} - [\eta_R - \Lambda^2 \gamma^2 \psi_R] \frac{dy(\xi)}{d\xi} - \beta_{TR} y(\xi) = 0 \quad (18)$$

The quadratic elastic coefficient of Pasternak foundation is given as:

$$k(\xi) = k_0(1 - \mu\xi^2), \quad \text{and} \quad g(\xi) = g_0(1 - \mu\xi^2), \quad (19)$$

where $k_0, g_0,$ and μ are constant values.

Substituting Eq. (19) into Eq. (14) and putting $\lambda = \Lambda^2$ hence, Eq. (14) becomes

$$\begin{aligned}
 & s(\xi) \frac{d^4 y(\xi)}{d\xi^4} + 2 \frac{ds(\xi)}{d\xi} \frac{d^3 y(\xi)}{d\xi^3} + \frac{d^2 s(\xi)}{d\xi^2} \frac{d^2 y(\xi)}{d\xi^2} + n(\xi) \frac{d^2 y(\xi)}{d\xi^2} + \frac{dn(\xi)}{d\xi} \frac{dy(\xi)}{d\xi} \\
 & + \lambda \gamma^2 \left[h(\xi) \frac{d^2 y(\xi)}{d\xi^2} + \frac{dh(\xi)}{d\xi} \frac{dy(\xi)}{d\xi} \right] - g_0 (1 - \mu \xi^2) \frac{d^2 y(\xi)}{d\xi^2} - \frac{dg(\xi)}{d\xi} \frac{dy(\xi)}{d\xi} \\
 & + \left[k_0 (1 - \mu \xi^2) - \lambda r(\xi) \right] y(\xi) = 0
 \end{aligned} \tag{20}$$

III. METHODOLOGY

A. Differential Transform Method (DTM)

The Differential Transform Method (DTM) is a robust analytical method derived from Taylor series expansion, primarily used to solve differential equations. Introduced by Zhou in 1986, DTM effectively addresses both linear and nonlinear equations, particularly in the field of electrical circuits. Through specific transformation rules, DTM changes differential equations and their boundary conditions into algebraic equations, representing the differential transforms of the original functions. By solving these algebraic equations, the method yields the expected solutions. Unlike traditional high-order Taylor series expansions, which require symbolic manipulation of differential coefficients, DTM provides a recursive approach to obtain higher-order solutions. This process ultimately leads to an exact solution expressed in algebraic form. Basic definition and operations of DTM are presented as follows.

The differential transformation of a function $g(x)$ is defined as:

$$\overline{G}(k) = \frac{1}{k!} \left[\frac{d^k g(t)}{dt^k} \right]_{t=0} \tag{21}$$

In Eq. (21), $g(t)$ is the original function and $\overline{G}(k)$ is the transformed function.

The inverse differential transform of $\overline{G}(k)$ is given as

$$g(t) = \sum_{k=0}^{\infty} \overline{G}(k) t^k \tag{22}$$

Utilizing Eqs. (21) and (22) yields

$$g(t) = \sum_{k=0}^{\infty} \frac{t^k}{k!} \left[\frac{d^k g(t)}{dt^k} \right]_{t=0} \tag{23}$$

which represents Taylor series of $g(t)$ at $t = 0$. Eq. (23) suggests that the idea of differential transformation is derived from the Taylor series expansion. In practical applications, the function $g(t)$ is expressed by a finite series and Eq. (23) is written as

$$g(t) = \sum_{k=0}^m \overline{G}(k) t^k \tag{24}$$

which implies that

$$g(t) = \sum_{k=m+1}^{\infty} \overline{G}(k) t^k \tag{25}$$

Herein, the convergence of the natural frequencies is a function of the value of m .

B. Application of Differential Transform Method

The differential transform method is used to solve the dimensionless form of equation of motion presented in Eq. (20), together with the corresponding boundary conditions outlined in Eqs. (15) – (18). This approach results in the derivation of a system of recurrence algebraic relations.

$$\begin{aligned}
 & \sum_{k=0}^w S(w-k)(k+1)(k+2)(k+3)(k+4)Y(k+4) \\
 & + 2 \sum_{k=0}^w (w-k+1)S(w-k+1)(k+1)(k+2)(k+3)Y(k+3) \\
 & + \sum_{k=0}^w (w-k+1)(w-k+2)S(w-k+2)(k+1)(k+2)Y(k+2) \\
 & + \sum_{k=0}^w N(w-k)(k+1)(k+2)Y(k+2) + \sum_{k=0}^w (w-k+1)N(w-k+1)(k+1)Y(k+1) \\
 & + \lambda\gamma^2 \sum_{k=0}^w H(w-k)(k+1)(k+2)Y(k+2) + \lambda\gamma^2 \sum_{k=0}^w (w-k+1)H(w-k+1)(k+1)Y(k+1) \\
 & - g_0(w+1)(w+2)Y(w+2) + \sum_{k=0}^w \mu g_0 \delta(w-k-2)(k+1)(k+2)Y(k+2) \\
 & + 2 \sum_{k=0}^w \mu g_0 \delta(w-k-1)(k+1)Y(k+1) + k_0 Y(w) - \sum_{k=0}^w \mu k_0 \delta(w-k-2)Y(k) \\
 & - \lambda \sum_{k=0}^w R(w-k)Y(k) = 0, \tag{26}
 \end{aligned}$$

where $Y(w), S(w), N(w), H(w)$ and $R(w)$ are the T-functions of $y(\xi), s(\xi), n(\xi), h(\xi)$ and $r(\xi)$ respectively.

At $\xi = 0$,

$$2Y(2) - \beta_{\theta L}Y(1) = 0 \tag{27}$$

and

$$\begin{aligned}
 & 6Y(3) + 2s'(0)Y(2) + n(0)Y(1) \\
 & + \lambda\gamma^2 h(0)Y(1) + \beta_{TL}Y(0) = 0 \tag{28}
 \end{aligned}$$

At $\xi = 1$,

$$\sum_{k=0}^m k(k-1)Y(k) + \beta_{\theta R} \sum_{k=0}^m kY(k) = 0 \tag{29}$$

$$Y(3) = -\frac{\beta_{TL}s}{6} - \left[\frac{\beta_{\theta L}s'(0)}{6} + \frac{n(0)}{6} + \frac{\lambda\gamma^2 h(0)}{6} \right] \tag{32}$$

Following the same recursive procedure, the m^{th} term $Y(m)$ can be determined. Substitute $Y(0)$ to $Y(m)$ into Eqs. (29) and (30) to give

Utilizing the differential transformation technique to Eqs. (15) – (18), we have

$$\begin{aligned}
 & \sum_{k=0}^m k(k-1)(k-2)Y(k) + \tau_R \sum_{k=0}^m k(k-1)Y(k) \\
 & - [\eta_R - \lambda\gamma^2 \psi_R] \sum_{k=0}^m kY(k) - \beta_{TR} \sum_{k=0}^m kY(k) = 0 \tag{30}
 \end{aligned}$$

Let $Y(0) = s$,

$Y(1) = z$,

such that s and z represent unknown values.

Solving Eqs. (27) and (28) gives

$$Y(2) = \frac{\beta_{\theta L}z}{2} \tag{31}$$

$$N_{j1}^{(m)}(\lambda)s + N_{j2}^{(m)}(\lambda)z = 0, \tag{33}$$

where $j = 1, 2, \dots$, $N_{j1}^{(m)}(\lambda)$, $N_{j2}^{(m)}(\lambda)$ are λ - polynomials associated with m .

As a result of Eq. (33), the frequency equation is expressed as follows:

$$\begin{vmatrix} N_{11}^{(m)}(\lambda) & N_{12}^{(m)}(\lambda) \\ N_{21}^{(m)}(\lambda) & N_{22}^{(m)}(\lambda) \end{vmatrix} = 0 \quad (34)$$

Solving Eq. (34), the dimensionless frequencies are determined with $\lambda = \Lambda^2$, to give $\Lambda = \Lambda_i^{(m)}$, $i =$

$1, 2, \dots$ where $\Lambda_i^{(m)}$ is the i^{th} expected natural frequency associated with m , where m is determined by the following criterion:

$$\left| \Lambda_i^{(m)} - \Lambda_i^{(m-1)} \right| \leq \varepsilon, \quad (35)$$

where $\Lambda_i^{(m-1)}$ is the i^{th} expected natural frequency associated with $m-1$ and ε is the convergence criterion. In this work, $\varepsilon = 0.0001$.

C. Numerical Analysis

To illustrate the theory of DTM, the natural vibration of an axially functionally graded tapered clamped-free and clamped-clamped beams on a quadratic Pasternak foundation are discussed. The mechanical characteristics of the beam are described as follows:

$$E(x) = E(0) \left(1 + \beta \frac{x}{l} \right) \quad (36)$$

$$A(x) = A(0) \left(1 - c \frac{x}{l} \right) \quad (37)$$

$$I(x) = I(0) \left(1 - c \frac{x}{l} \right)^3 \quad (38)$$

$$N(x) = \int_x^l \rho(\xi) A(\xi) \Omega^2 \xi d\xi$$

$$= \rho(0) A(0) \Omega^2 l^2 \left[\frac{1}{2} + \frac{1}{3}(a-c) + \frac{1}{4}(b-ac) - \frac{1}{5}bc - \frac{\xi^2}{2} + \frac{1}{3}(c-a)\xi^3 + \frac{1}{4}(ac-b)\xi^4 + \frac{1}{5}bc\xi^5 \right] \quad (40)$$

Also,

$$s(\xi) = 1 + (\beta - 3c)\xi + 3(c^2 - c\beta)\xi^2 + (3c^2\beta - c^3)\xi^3 - \beta c^3\xi^4 \quad (41)$$

$$r(\xi) = 1 + (a - c)\xi + (b - ac)\xi^2 - bc\xi^3 \quad (42)$$

$$h(\xi) = 1 + (a - 3c)\xi + (b - 3ac + 3c^2)\xi^2 + (3ac^2 - 3bc - c^3)\xi^3 + (3bc^2 - ac^3)\xi^4 - bc^3\xi^5 \quad (43)$$

$$n(\xi) = -\alpha^2 \left[\frac{1}{2} + \frac{1}{3}(a-c) + \frac{1}{4}(b-ac) - \frac{1}{5}bc - \frac{\xi^2}{2} + \frac{1}{3}(c-a)\xi^3 + \frac{1}{4}(ac-b)\xi^4 + \frac{1}{5}bc\xi^5 \right] \quad (44)$$

$$\rho(x) = \rho(0) \left[1 + a \left(\frac{x}{l} \right) + b \left(\frac{x}{l} \right)^2 \right] \quad (39)$$

where $E(0)$, $I(0)$, $\rho(0)$ and $A(0)$ are Young's modulus, moment of inertia, mass per unit volume and cross section area at $x = 0$ respectively and β , a , b , c are some constant values. Computer codes derived with MAPLE 18 using Eqs (26) - (30) were used to compute the dimensionless frequencies for $\gamma = 0.01$, $k_0 = 10$, $g_0 = 2$, $c = 0.5$, $a = 1$, $b = 1$, $\alpha = 5$, $\beta = 0.5$, $\mu = 0.1$, and $\beta_{TR} = \beta_{TL} = \beta_{\theta R} = \beta_{\theta L} = 0$.

IV. RESULTS AND DISCUSSION

The first six dimensionless frequencies λ_1 to λ_6 were analyzed for beams under clamped-free and clamped-clamped boundary conditions. The dimensionless frequencies demonstrated smooth and sequential convergence, with no missing modes, highlighting the robustness of the computational method. The convergence analysis revealed intriguing trends in the vibrational characteristic of axially functionally graded (AFG) tapered Rayleigh beams on a quadratic Pasternak elastic subgrade. Notably, the clamped-free boundary condition exhibited faster convergence of the first six dimensionless frequencies compared to the clamped-clamped configuration. However, the frequencies of the clamped-free beams were consistently lower than those observed for their clamped-clamped counterparts, reflecting the effect of boundary constraints on the stiffness and vibrational response of the beams. Tables 1, 2, 4 and 5 are presented to examine the influences of inverse of the slenderness ratio, axial force and quadratic elastic foundation on the first three dimensionless frequencies of a clamped-free and clamped-clamped beam under consideration.

A. Clamped-Free Beam

Figures 2 and 3 show the convergence the first six dimensionless frequencies of a clamped-free AFG tapered Rayleigh beam λ_1 to λ_6 converge to 6.5006, 19.9823, 44.6309, 80.8282, 128.6100, 187.9219 for $\varepsilon = 0.0001$, the corresponding number of terms (m) are 32, 34, 35, 36, 78, and 88 respectively. This demonstrates the reliability and precision of the computational approach in capturing the beam's dynamic behaviour.

Figures 4–6 illustrate the 1st–3rd mode shapes for axially graded and axially non-graded tapered Rayleigh beams on quadratic elastic foundations. The analysis reveals notable differences in the vibrational behaviour of these two beam types, emphasizing the influence of material gradation on vibration characteristic, which softens the beam in certain regions, allowing for greater flexibility and deformation with the axially non-graded tapered Rayleigh beam showing more rigid behaviour. The FG tapered Rayleigh beam with larger displacements at lower dimensionless frequencies, indicating reduced overall stiffness compared to non-graded tapered Rayleigh beam. The non-graded tapered Rayleigh beam which shows more rigid behaviour, with smaller displacements across all mode shapes, reflecting the uniform distribution of material properties that enhances structural stiffness. For FG tapered Rayleigh

Tables 1 and 2 present the influence of the inverse of slenderness ratio (γ), axial force (α), and quadratic Pasternak foundation on the dimensionless frequencies. It is observed that an increase in the inverse slenderness ratio reduces the dimensionless frequencies, indicating a decrease in stiffness as the beam becomes relatively slender. Whereas, an increase in axial force leads to higher dimensionless frequencies, reflecting the stiffening effect of axial tension on the beam's vibrational characteristics. Additionally, the effect of the Winkler foundation (k_0) becomes apparent when the shear modulus (g_0) is set to zero. In this case, the dimensionless frequencies increase with higher values of the Winkler modulus, emphasizing its role in providing additional support. The introduction of the Pasternak foundation further increases the dimensionless frequencies due to the shear interaction. However, a notable exception is observed for the first dimensionless frequency (λ_1), where the combined Pasternak-Winkler foundation results in a frequency reduction. This unexpected phenomenon is unique to the clamped-free boundary condition and warrants further investigation.

Table 3 compares the dimensionless frequencies for axially functionally graded and axially non-functionally graded tapered Rayleigh beams for a clamped-free boundary condition on a quadratic elastic foundation. For the axially non-graded tapered Rayleigh ($a = 0, b = 0, \beta = 0$), the frequencies are higher than those of the axially graded tapered Rayleigh beam. This suggests that the functional grading of material properties, while beneficial for specific performance objectives, results in reduced frequencies compared to uniform material distribution.

beam, it was observed in Figures 4 and 5 that the 1st and 2nd mode shapes display significantly larger displacements in the range $0 \leq \xi \leq 1$ at lower dimensionless frequencies. This pattern highlights the pronounced effect of material gradation in regions where the foundation's support is less dominant, allowing the beam to vibrate more freely. In Figure 6, the third mode shape of FG beam shows larger displacements across most of the domain $0 \leq \xi \leq 1$, except in the localized region where $0.52 \leq \xi \leq 0.70$. Within this interval, the displacement of the FG tapered Rayleigh beam is reduced compared to other regions, possibly due to localized stiffness effects caused by the material gradation or the interaction with the quadratic elastic foundation.

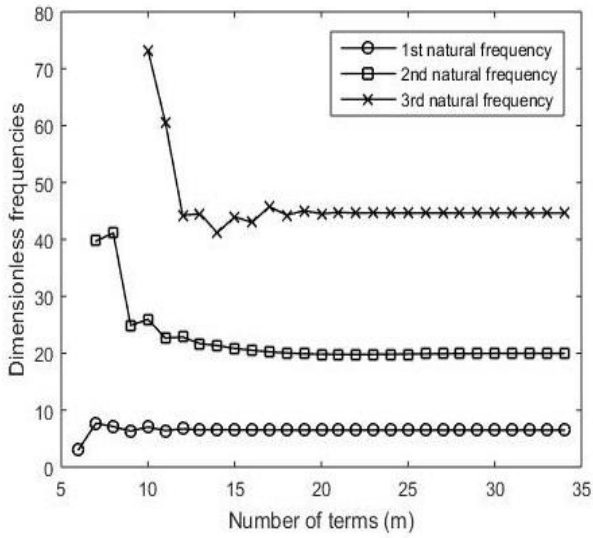


Figure 2: The convergence curve for 1st, 2nd and 3rd dimensionless frequencies

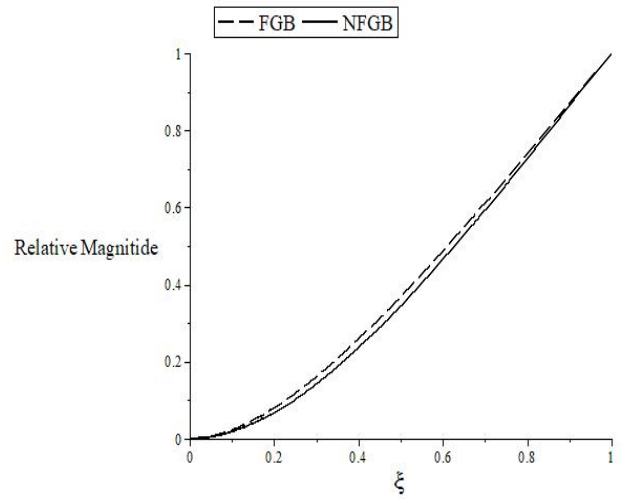


Figure 4: Comparison of the 1st mode shape of FGB and NFG

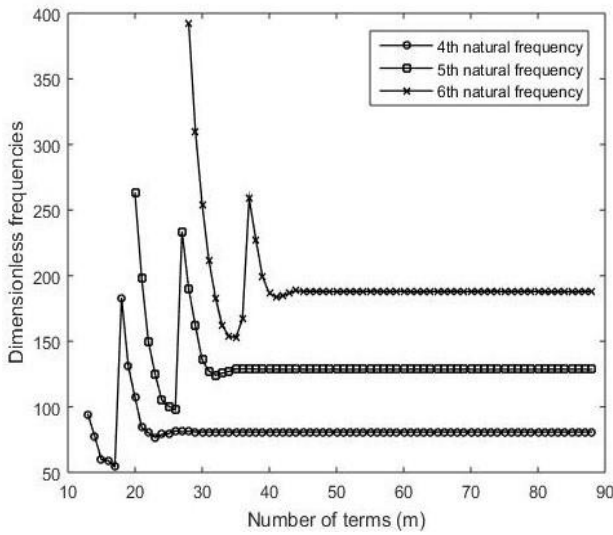


Figure 3: The convergence curve for 4th, 5th and 6th dimensionless frequencies

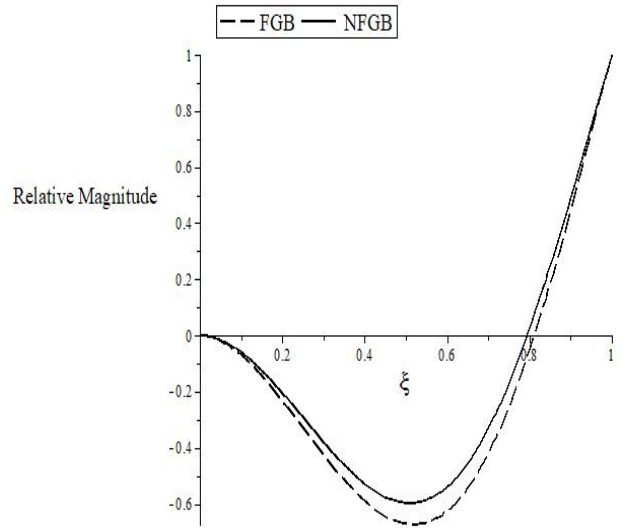


Figure 5: Comparison of the 2nd mode of FGB and NFG

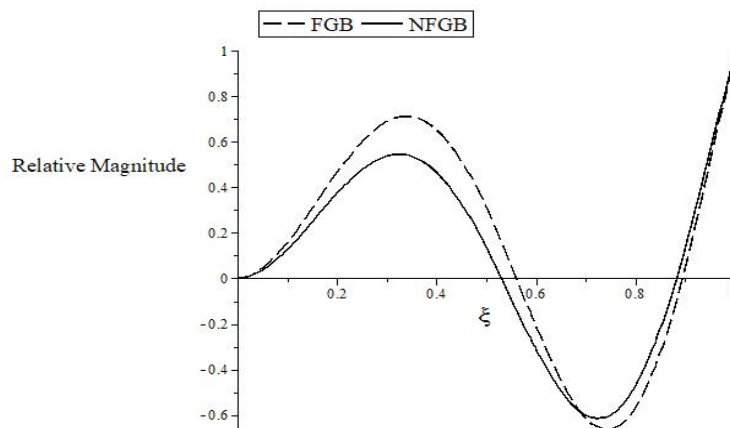


Figure 6: Comparison of the 3rd mode shape of FGB and NFG

Table 1: Effects of the inverse of slenderness ratio (γ), and quadratic elastic foundation on dimensionless frequencies

γ	Pasternak		$g_0 = 0$			$g_0 = 5$			$g_0 = 10$		
	λ	Winkler	k_0			k_0			k_0		
			0	200	400	0	200	400	0	200	400
0.0000	λ_1		6.0325	12.8501	17.1290	5.9373	12.7666	17.0396	5.8908	12.7147	16.9800
	λ_2		19.3614	22.6891	25.5922	20.4763	23.6665	26.4782	21.5212	24.5900	27.3182
	λ_3		43.8516	45.4803	47.0539	45.7594	47.3245	48.8406	47.5831	49.0921	50.5570
0.0100	λ_1		6.0315	12.8480	17.1261	5.9364	12.7644	17.0365	5.8898	12.7125	16.9769
	λ_2		19.3478	22.6732	25.5743	20.4617	23.6498	26.4595	21.5058	24.5724	27.2988
	λ_3		43.7773	45.4033	46.9744	45.6817	47.2443	48.7580	47.5023	49.0086	50.4711
0.0130	λ_1		6.0310	12.8469	17.1244	5.9358	12.7632	17.0348	5.8892	12.7112	16.9751
	λ_2		19.3401	22.6643	25.5642	20.4536	23.6404	26.4491	21.4971	24.5626	27.2880
	λ_3		43.7357	45.3602	46.9299	45.6381	47.1993	48.7117	47.4570	48.9621	50.4231
0.0200	λ_1		6.0287	12.8417	17.1173	5.9335	12.7579	17.0274	5.8869	12.7058	16.9675
	λ_2		19.3071	22.6257	25.5208	20.4183	23.5998	26.4039	21.4596	24.5200	27.2409
	λ_3		43.5567	45.1748	46.7384	45.4511	47.0062	48.5126	47.2621	48.7612	50.2167
0.0250	λ_1		6.0266	12.8370	17.1107	5.9313	12.7530	17.0206	5.8847	12.7009	16.9606
	λ_2		19.2768	22.5902	25.4809	20.3859	23.5625	26.3624	21.4252	24.4809	27.1978
	λ_3		43.3934	45.0058	46.5638	45.2805	46.8300	48.3310	47.0844	48.5781	50.0284

Table 2: Effect axial force (α) on dimensionless frequencies for $\gamma = 0.01$

α	Pasternak		$g_0 = 0$			$g_0 = 5$			$g_0 = 10$		
	λ	Winkler	k_0			k_0			k_0		
			0	200	400	0	200	400	0	200	400
0	λ_1		2.5691	11.5791	16.1542	2.1429	11.4373	16.0198	1.9905	11.3720	15.9498
	λ_2		14.2068	18.5074	21.9894	15.7994	19.7857	23.0971	17.1962	20.9365	24.1045
	λ_3		38.2474	40.1039	41.8802	40.4248	42.1879	43.8817	42.4834	44.1662	45.7885
5	λ_1		6.0315	12.8480	17.1261	5.9364	12.7644	17.0365	5.8898	12.7125	16.9769
	λ_2		19.3478	22.6732	25.5743	20.4617	23.6498	26.4595	21.5058	24.5724	27.2988
	λ_3		43.7773	45.4033	46.9744	45.6817	47.2443	48.7580	47.5023	49.0086	50.4711
10	λ_1		10.9335	15.7930	19.4690	10.9181	15.7645	19.4319	10.9092	15.7426	19.4016
	λ_2		29.7815	32.0304	34.1328	30.4272	32.6383	34.7101	31.0642	33.2390	35.2812
	λ_3		57.0512	58.3008	59.5239	58.5001	59.7202	60.9181	59.9102	61.1027	62.2739

Table 3: Comparison of the dimensionless frequencies of Functionally Graded Beam (FGB) and Non- Functionally Graded Beam (NFGB)

Dimensionless frequency	FGB	NFGB
λ_1	6.5004	7.7005
λ_2	19.9789	22.9141
λ_3	44.6311	52.1741

B. Clamped-Clamped Beam

Figures 7 and 8 demonstrate the convergence the first six dimensionless frequencies λ_1 to λ_6 of a clamped-clamped AFG tapered Rayleigh beam. These frequencies converge to 17.2786, 42.8628, 79.3745, 127.3212,

187.0677, 253.6675 for $\varepsilon = 0.0001$, with the corresponding number of terms (m) being 34, 36, 38, 50, 78, and 90 respectively. Notably, the dimensionless frequencies of the C-C beam are significantly higher than those of the clamped-free (C-F) beam on the same

quadratic Pasternak foundation. This difference is as a result of the C-C boundary condition, which imposes additional rotational constraints at both ends of the beam, thereby increasing its stiffness and elevating its natural frequencies.

Tables 4 and 5 show the influence of the inverse of slenderness ratio (γ), axial force (α), and quadratic Pasternak foundation on the dimensionless frequencies of a C-C FG tapered Rayleigh beam. It was observed that increasing the inverse of the slenderness ratio (γ) reduces the dimensionless frequencies (λ). Higher axial force (α) increases the dimensionless frequencies. The addition of a Winkler foundation increases the dimensionless frequencies. Introducing the Pasternak parameter further elevates the frequencies. Table 6 compares the dimensionless frequencies of FG and non-graded tapered Rayleigh beams on a quadratic Pasternak foundation.

The frequencies of the non-FG beam are higher than those of the FG beam, reflecting the greater stiffness of

the non-graded beam due to its uniform material properties.

Figures 9 – 11 show comparisons of the 1st – 3rd mode shapes of an axially functionally graded tapered Rayleigh beam and axially non-functionally graded tapered Rayleigh beam on quadratic elastic foundation. In Figure 9, for the non-FG beam, the 1st mode shape exhibits larger displacements within the range $0.3 \leq \xi \leq 0.8$, corresponding to higher frequencies. This behaviour contrasts with the C-F boundary condition, where FG beam typically exhibits larger displacements at lower frequencies. In Figure 10, the non-FG tapered Rayleigh beam displays larger displacements for $0.54 \leq \xi \leq 0.8$, further emphasizing the higher stiffness of the non-graded beam. In Figure 11, for the non-graded beam, larger displacements occur in the intervals $0.4 \leq \xi \leq 0.54$ and $0.68 \leq \xi \leq 0.88$. These localized differences highlight the impact of material grading on higher-order mode shapes, where the dynamic response becomes increasingly complex.

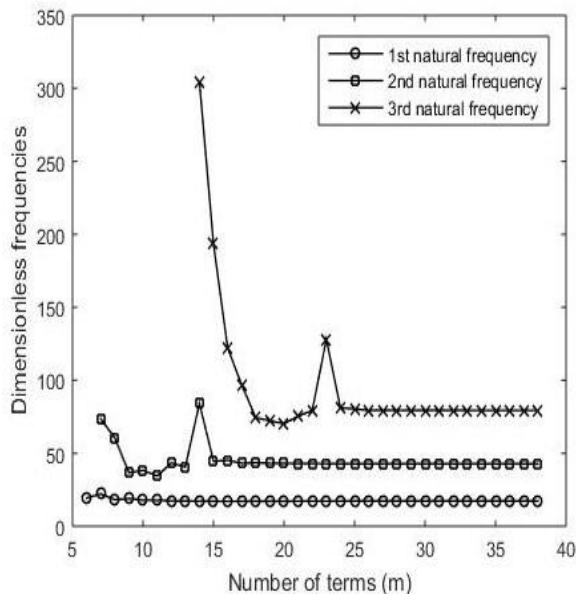


Figure 7: The convergence curve for 1st, 2nd and 3rd dimensionless frequencies

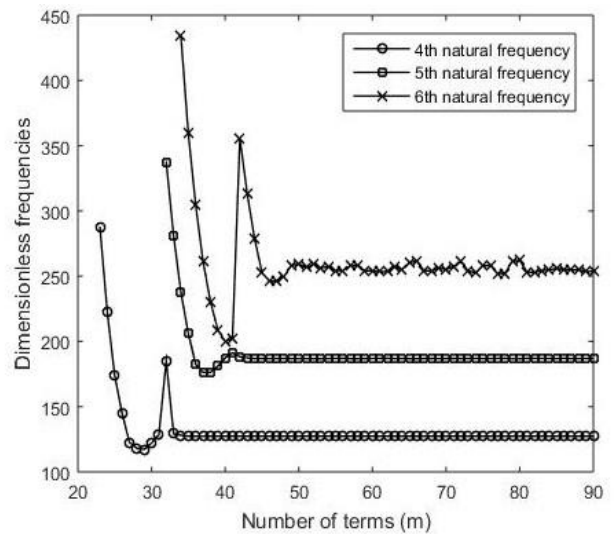


Figure 8: The convergence curve for 1st, 2nd and 3rd dimensionless frequencies

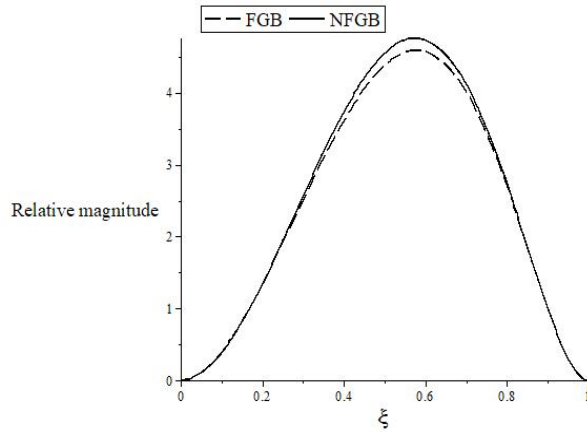


Figure 9: Comparison of the 1st mode shape of FGB and NFGT

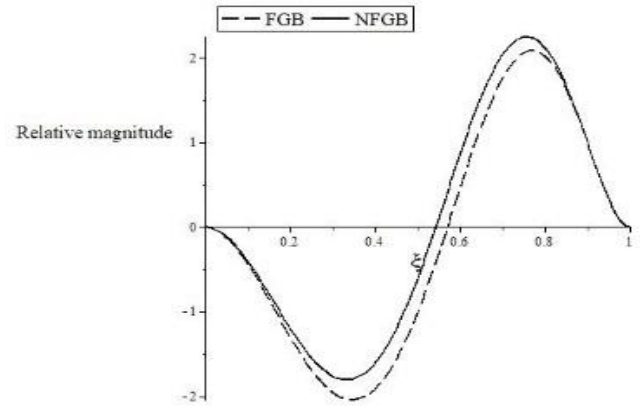


Figure 10: Comparison of the 2nd mode shape of FGB and NFGT

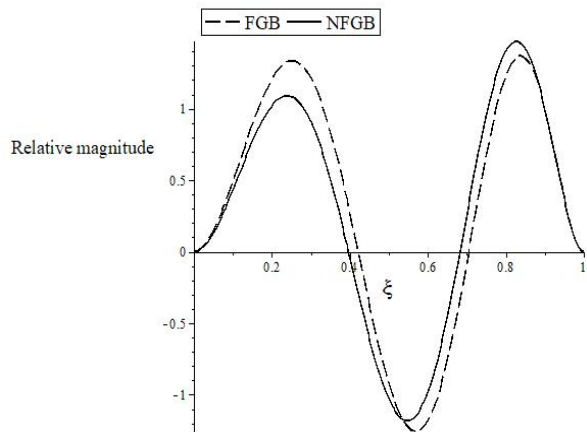


Figure 11: Comparison of the 3rd mode shape of FGB and NFGT

Table 4: Effects of the inverse of slenderness ratio (γ), and quadratic elastic foundation on dimensionless frequencies

γ	Pasternak Winkler λ	$g_0 = 0$			$g_0 = 5$			$g_0 = 10$		
		k_0			k_0			k_0		
		0	200	400	0	200	400	0	200	400
0.0000	λ_1	16.5464	20.4467	23.7100	17.8303	21.5026	24.6298	19.0173	22.4997	25.5078
	λ_2	42.0216	43.7372	45.3891	44.0059	45.6473	47.2326	45.8972	47.4736	49.0003
	λ_3	78.5907	79.5268	80.4535	80.9200	81.8293	82.7309	83.1819	84.0669	84.9418
0.0100	λ_1	16.5417	20.4409	23.7032	17.8253	21.4965	24.6228	19.0119	22.4934	25.5007
	λ_2	41.9725	43.6862	45.3361	43.9546	45.5941	47.1777	45.8439	47.4185	48.9433
	λ_3	78.3900	79.3237	80.2469	80.7126	81.6204	82.5181	82.9697	83.8524	84.7267
0.0130	λ_1	16.5390	20.4376	23.6994	17.8224	21.4931	24.6189	19.0089	22.4898	25.4967
	λ_2	41.9450	43.6575	45.3063	43.9258	45.5643	47.1468	45.8140	47.3875	48.9115
	λ_3	78.2770	79.2102	80.1328	80.5974	81.5043	82.4003	82.8496	83.7327	84.6039
0.0200	λ_1	16.5275	20.4234	23.6830	17.8102	21.4783	24.6020	18.9959	22.4745	25.4792
	λ_2	41.8262	43.5338	45.1781	43.8018	45.4356	47.0137	45.6850	47.2541	48.7737
	λ_3	77.7958	78.7234	79.6399	80.1023	81.0035	81.8940	82.3419	83.2182	84.0861
0.0250	λ_1	16.5170	20.4103	23.6678	17.7989	21.4647	24.5863	18.9840	22.4603	25.4632
	λ_2	41.7174	43.4207	45.0606	43.6882	45.3178	46.8918	45.5668	47.1319	48.6475
	λ_3	77.3598	78.2817	79.1930	79.6541	80.5500	81.4346	81.8811	82.7532	83.6146

Table 5: Effect axial force (α) on dimensionless frequencies for $\gamma = 0.01$

α	Pasternak Winkler	$g_0 = 0$			$g_0 = 5$			$g_0 = 10$		
		k_0			k_0			k_0		
		λ	0	200	400	0	200	400	0	200
0	λ_1	2.5691	11.5791	16.1542	2.1429	11.4373	16.0198	1.9905	11.3720	15.9498
	λ_2	14.2068	18.5074	21.9894	15.7994	19.7857	23.0971	17.1962	20.9365	24.1045
	λ_3	38.2474	40.1039	41.8802	40.4248	42.1879	43.8817	42.4834	44.1662	45.7885
5	λ_1	6.0315	12.8480	17.1261	5.9364	12.7644	17.0365	5.8898	12.7125	16.9769
	λ_2	19.3478	22.6732	25.5743	20.4617	23.6498	26.4595	21.5058	24.5724	27.2988
	λ_3	43.7773	45.4033	46.9744	45.6817	47.2443	48.7580	47.5023	49.0086	50.4711
10	λ_1	10.9335	15.7930	19.4690	10.9181	15.7645	19.4319	10.9092	15.7426	19.4016
	λ_2	29.7815	32.0304	34.1328	30.4272	32.6383	34.7101	31.0642	33.2390	35.2812
	λ_3	57.0512	58.3008	59.5239	58.5001	59.7202	60.9181	59.9102	61.1027	62.2739

Table 6: Comparison of the dimensionless frequencies of Functionally Graded Beam (FGB) and Non-Functionally Graded Beam (NFGB)

Non-dimensional frequency	FGB	NFGB
λ_1	17.2784	19.7222
λ_2	42.8630	49.5099
λ_3	79.3749	92.9390

Table 7: Comparison of the first three dimensionless frequencies of a clamped-clamped uniform Rayleigh beam for a constant elastic foundation

γ	k_0	$g_0 = 0$			$g_0 = 5$			$g_0 = 10$		
		Present	Adair et al. (2018)	De Rosa and Maurizi (1998)	Present	Adair et al. (2018)	De Rosa and Maurizi (1998)	Present	Adair et al. (2018)	De Rosa and Maurizi (1998)
1	0	22.3725	22.3733	22.3729	23.7035	23.6877	23.7072	28.3531	28.2971	28.3024
		61.6646	61.6728	61.6853	63.5017	63.4890	63.4890	70.3393	70.2445	70.2244
		120.8689	120.903	120.9120	122.8960	122.8000	122.8993	130.6819	130.4850	130.6449
416	10000	102.469	102.454	102.475	102.767	102.759	102.759	103.938	103.918	103.917
		117.473	117.462	117.484	118.448	118.418	118.440	122.249	122.189	122.213
		156.855	156.775	156.901	158.463	158.332	158.458	164.536	164.352	164.481

C. Validation of results with those documented in existing literature

The method used was validated using a clamped-clamped uniform Rayleigh beam on a constant Pasternak elastic foundation. This was achieved by setting the taper ratio (c), as well as the constants a , b , μ and β , in the governing equation of an axially functionally graded tapered Rayleigh beam on a quadratic Pasternak foundation support, to zero. Table 7 presents the DTM results for the first three dimensionless frequencies of the clamped-clamped beam. The comparison revealed a strong correlation between the DTM outcomes and previously reported values, demonstrating the accuracy and reliability of the method.

V. CONCLUSION

In this work, the DTM was utilized to find closed-form series solutions for the natural vibration problem of an axially functionally graded (AFG) tapered Rayleigh beam on a bi-parametric foundation, incorporating quadratic Pasternak foundations. Beams on elastic foundations are extensively utilized in structural engineering applications, including bridge decks, high-rise buildings, offshore platforms, and wind turbine towers. The results provided valuable insights into how vibration characteristics of a structure varied with changes in foundation parameters and the influence of rotatory inertia. The research findings offered practical applications for investigating vibration behaviour in aerospace structures and modelling complex multi-layered

systems commonly encountered in engineering. Furthermore, these findings proved beneficial for analyzing the seismic response of beams on elastic foundations, contributing to the early detection of structural weaknesses and the prevention of permanent damage caused by vibration effects. By examining the phase differences between mode shapes, the study enhanced the understanding of complex vibration behaviour, enabling more informed decisions in the design, troubleshooting, and enhancement of beams for multifarious engineering practices. This was particularly relevant in scenarios involving boundary constraints and foundation interactions. The key findings of this research can be summarized as follows:

- (i) the Winkler foundation stiffness parameter has a direct influence on the dimensionless frequencies in a positive manner, causing them to increase;
 - (ii) higher Shear stiffness properties led to a corresponding increase in dimensionless frequencies;
 - (iii) dimensionless frequencies increased with increasing axial force, indicating a stiffening effect;
 - (iv) the Pasternak foundation parameter had a more significant influence on dimensionless frequencies compared to the Winkler foundation parameter, as beams resting on Pasternak foundations exhibited higher dimensionless frequencies; and
 - (v) axially non-functionally graded tapered Rayleigh beams on elastic foundations demonstrated higher dimensionless frequencies due to their uniform material properties and a more consistent stiffness- to- mass ratio.
- Further studies on non-uniform FG plates and shells under dynamic loads, optimize design strategies for FG structures used in bridges, robotic arms, and biomedical implants, and utilize the findings in the design and analysis of tall buildings, bridges, and other civil infrastructure are recommended.

AUTHOR CONTRIBUTIONS

O. T. Olotu: Conceptualization, investigation and validation. **E. O. Omole:** Writing the original draft, review and editing. **R. O. Folaranmi:** Formal analysis and funding acquisition. **B. M. Yisa:** Research administration and methodology. **P. O. Adeniran:** Software development. **J. A. Gbadeyan:** Supervision.

REFERENCES

Adair, D., Ismailov, K., and Jaeger, M. (2018). Vibration of a Beam on an Elastic Foundation Using the Variational Iteration Method. *International Journal of Aerospace and Mechanical Engineering*, 12(9), 914-919.

Alshorbagy, A. E., Eltahir, M. A., and Mahmoud, F. F. (2011). Free vibration characteristics of functionally graded beams using finite element approach. *Journal of Theoretical and Applied Mechanics*, 49(2), 321-339.

Avcar, M., and Alsaid, S. S. (2017). Free vibration analysis of Rayleigh beam composed of functionally graded materials considering simply-supported boundary

conditions. *Journal of Vibration and Control*, 23(12), 2026-2044.

Aydogdu, M., and Taskin, M. (2007). Free vibration analysis of functionally graded beams using Navier solution method. *Composite Structures*, 80(1), 45-53.

Catal, S. (2008). Solution of free vibration equations of beam on elastic soil by using differential transform method. *Applied Mathematical Modeling*, 32(9), 1744-1757.

Chen, Y. F., Zang, Z. P., Dong, S. H., Ao, C., Liu, H., Ma, S., ... and Feng, W. (2021). Flapwise bending vibration analysis of rotating tapered Rayleigh beams for the application of offshore wind turbine blades. *China Ocean Engineering*, 35(4), 544-553.

Coskun, I., Ozturk, M., and Mutman, U. (2014). Vibration analysis of non-uniform Euler-Bernoulli beam on elastic foundations using Adomain Decomposition Method. *Journal of Sound and Vibration*, 333(5), 1490-1506.

De Rosa, M. A., and Maurizi, M. J. (1998). The influence of concentrated masses and Pasternak soil on the free vibrations of Euler beam - Exact solution. *Journal of Sound and Vibration*, 212(4), 573-581.

Ebrahimi-Mamaghani, A., Sarparast, M., and Rezaei, M. (2020). Free and forced vibration analysis of axially functionally graded Rayleigh and Euler-Bernoulli beams moving under load. *Journal of Solid Mechanics*, 12(2), 429-447.

Kumar, S. (2022). Natural frequencies of beams with axial material gradation resting on two parameter elastic foundation. *Trends in Sciences*, 19(6), 3048-3058.

Lamprea-Pineda, A. C., Connolly, D. P., and Hussein, M. F. (2022). Beams on elastic foundations—A review of railway applications and solutions. *Transportation Geotechnics*, 33, 1-63.

Lazreg, H. and Fabrice, B. (2020). Bending and free vibration analysis of functionally graded beams on elastic foundations with analytical validation. *Advances in Materials Research*, 9(1) 63-98.

Ma, J., Wang, J., Wang, C., and Guo Y., (2024). Vibration response of beams-supported by finite-thickness elastic foundation under a concentrated force. *Journal of Mechanical Science and Technology*, 38, 595-604.

Ma J., Li, D., Yang, H., Wang, J., Wang, C., and Guo, Y., (2024). Analytical investigation on the dynamic behavior of multi-span continuous beams supported on soil with finite depth. *Coatings*, 14, 1-16.

Malik, M., and Dang, V. (1998). Structural dynamics: differential transform method and its applications. *Computer Modeling in Engineering & Sciences*, 1(1), 73-88.

Mei, C. (2008). Free lateral vibrations of centrifugally stiffened rotating Euler-Bernoulli beam using the differential transform method. *Journal of Sound and Vibration*, 318(1-2), 397-412.

Olotu, O. T., Gbadeyan, J. A., and Agboola, O. O. (2023). Free Vibration Analysis of Tapered Rayleigh Beams resting on Variable Two-Parameter Elastic Foundation. *Forces in Mechanics*, 12, 1-12.

Shahba, A., Attarnejad, R., Marvi, A., and Hajilar, S. (2011). Finite element analysis of free vibration and stability of functionally graded Timoshenko beams. *European Journal of Mechanics-A Solids*, 30(2), 274-283.

Simsek, M. (2010). Fundamental frequency analysis of functionally graded beams using higher-order beam theories. *Composite Structures*, 92(5), 1220-1230.

Skalba, P., and Liskiewicz, A. (2018). Natural frequencies of beams with axial material gradation resting on two parameter elastic foundation. *Trends in Sciences*, 11(1), 107-114.

Sulaiman M.A., Usman M.A., Mustapha R.A., Hammed F.A. and Raheem T.L., (2024). Effect of R coefficient of viscous damping on dynamic analysis of Euler-Bernoulli beam resting on elastic foundation using Integral Numerical Method. *J. Appl. Sci. Environ. Manage*, 28(3), 883-887, <https://www.ajol.info/index.php/jasem>.

Lohar, H., Mitra, A., and Sahoo, S., (2016). Free vibration analysis of axially functionally graded linearly taper beam on elastic foundation. In IOP Conference Series: *Materials Science and Engineering*, 149(1), 3-8.

Wattanasakulpong, N. (2012). Free vibration of functionally graded beams with general elastically end constraints using differential transform method. *Journal of Mechanical Science and Technology*, 26(12), 3951-59.